Hindawi Publishing Corporation
Mathematical Problems in Engineering
Volume 2013, Article ID 840648, 9 pages
http://dx.doi.org/10.1155/2013/840648

Research Article

Power-Split Hybrid Electric Vehicle Energy Management Based on Improved Logic Threshold Approach

Zhumu Fu,[1,2] Bin Wang,[1] Xiaona Song,[1] Leipo Liu,[1] and Xiaohong Wang[1]

[1] *Information Engineering College, Henan University of Science and Technology, Luoyang 471023, China*
[2] *School of Control Science and Engineering, Shandong University, Jinan 250061, China*

Correspondence should be addressed to Zhumu Fu; fzm1974@163.com

Received 22 July 2013; Revised 3 November 2013; Accepted 6 November 2013

Academic Editor: Baoyong Zhang

We design an improved logic threshold approach of energy management for a power-split HEV assisted by an integrated starter generator (ISG). By combining the efficiency map and the optimum torque curve of internal combustion engine (ICE) with the state of charge (SOC) of batteries, the improved logic threshold controller manages the ICE within its peak efficiency region at first. Then the electrical power demand is established based on the ICE energy output. On that premise, a variable logic threshold value K is defined to achieve the power distribution between the ISG and the electric motor/generator (EMG). Finally, simulation models for the power-split HEV with improved logic threshold controller are established in ADVISOR. Compared to the equally power-split HEV with the logic threshold controller, when using the improved logic threshold controller, the battery power consumption, the ICE efficiency, the fuel consumption, and the motor driving system efficiency are improved.

1. Introduction

To improve the efficiency and fuel economy of hybrid electric vehicle (HEV), many researchers focus on power-split HEVs [1–5] as they can achieve a potential of higher fuel economy and reduce the electrical system loss. The power-split hybrid system, which usually uses an ICE with integrated starter generator (ISG) [6, 7] and an electric motor/generator (EMG), combines the benefits of both the parallel- and series-type hybrid systems without the cost effectiveness of this hybrid system.

Since the structure of power-split HEV is more complicated [5, 8], traditional control methods (such as optimal control [9] and robust control [10]) cannot deal with this kind of system efficiently. So it needs a sophisticated control system to manage the power-split HEV power trains. Such control system requires a reasonable control strategy at first to improve the fuel-saving capability of the ICE, (see [11, 12]). To solve this problem, studies such as logic threshold approach applied to the design of the control strategy for HEV have been used to achieve the power or torque distribution [2, 13]. However, due to the individual characters of the power-split HEVs [5] and even different driving performance under different driving cycles to the same power-split HEV [14, 15], it is necessary to consider the individual ICE, structure, and other driving conditions like SOC and vehicles' speed of the HEV when designing the control strategy [16].

In this case, by analyzing the structure of a power-split HEV and its operation, we have designed an improved logic threshold controller to achieve the power distribution in the ICE and electrical system. Furthermore, to obtain the actual torque distributed in electrical system, a variable logic threshold value K is defined to achieve the power distribution between the ISG and the EMG. The improved logic threshold controller behaviors in simulation under different driving conditions are compared with the performances of logic threshold controller system. Results clearly demonstrate that the improved logic threshold approach can significantly improve the efficiency of the ICE and electrical system behavior.

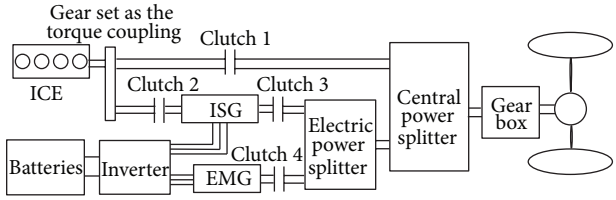

Figure 1: Structure of power-split HEV.

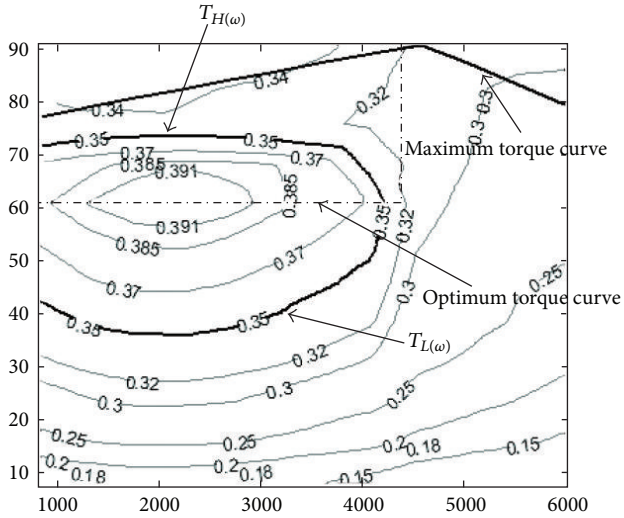

Figure 2: Efficiency map of an operating ICE.

2. Power-Split HEV Structure and Its Operation with Logic Threshold Approach

The structure of power-split HEV studied [5] is shown in Figure 1. To reduce inefficiencies of a single motor driving system, the power-split HEV adopts two motors in its electrical system, and that is, the ISG and the EMG. The former is integrated with the ICE by a gear set and the latter is downsized and integrated with the ISG and the ICE. Both of them can work as driving motor and generator. Since this structure increases the complexity of the electrical system, an electric power splitter and a central power splitter are used in it. To insure the independences of the ICE, the ISG, and the EMG, it adds the clutches 1–4.

To meet the power demand, the central power splitter distributes the power between the ICE and the electrical system and the electrical power splitter distributes the power between the ISG and the EMG. How to distribute the power among the ICE, the ISG, and the EMG is very important, so the main objective is to obtain the highest efficiency of the ICE. Figure 2 shows the efficiency map of an ICE, of which the maximum torque curve represents the highest ICE torque achievable for any speed. The contours show constant efficiencies, whose value will increase toward inner contours, so the points in dashed line are the highest efficiency operating points of the ICE at any corresponding speed. The dashed line can be called the ICE optimum torque curve. Notice that the ICE optimum torque curve must be limited within its peak efficiency region ($\eta_{\text{ICE}} \geq 0.35$), or else the optimal ICE output torque will change suddenly.

When driving the power-split HEV, ICE optimum torque curve can be used as a logic threshold value and ICE is operating at the optimum torque curve. By neglecting energy losses, the relationship among the ICE, the ISG, and the EMG can be expressed as

$$\begin{aligned} k_1 T_{\text{isg}} = T_{\text{ele}} = T_{\text{ice}}^{\text{req}} - T_{\text{ice}}^{\text{opt}}, \quad T_{\text{ice}}^{\text{opt}} > T_{\text{ice}}^{\text{req}} > 0, \\ k_1 T_{\text{isg}} + k_2 T_{\text{emg}} = T_{\text{ele}} = T_{\text{ice}}^{\text{req}} - T_{\text{ice}}^{\text{opt}}, \quad \text{else}, \end{aligned} \tag{1}$$

$$\begin{aligned} \omega_{\text{isg}} = k_1 \omega_{\text{ice}}, \qquad \omega_{\text{emg}} = k_2 \omega_{\text{ice}}, \qquad T_{\text{ice}}^{\text{opt}} \neq 0, \\ k_2 \omega_{\text{isg}} = k_1 \omega_{\text{emg}}, \qquad T_{\text{ice}}^{\text{opt}} = 0, \end{aligned} \tag{2}$$

where T_{isg} is the output torque from the ISG; T_{ele} is the output torque of the electrical system; $T_{\text{ice}}^{\text{req}}$ is the torque demand on the ICE; $T_{\text{ice}}^{\text{opt}}$ is the optimum output torque of the ICE, when the ICE is stopped; $T_{\text{ice}}^{\text{opt}} = 0$; T_{emg} is the output torque from the EMG; k_1 and k_2 are the gear ratios; ω_{isg} is the speed demand on the ISG; ω_{ice} is the actual speed of the ICE, which depends on the power-split HEV speed and the gear ratios; ω_{emg} is the speed demand on the EMG.

Equations (1) and (2) reflect the relationship between the ICE, the ISG, and the EMG when driving the power-split HEV. It is easy to calculate the power distribution of every component on the basis of obtaining the torque and speed. For instance, the optimum output power $P_{\text{ice}}^{\text{opt}}$ from the ICE can be calculated by using $T_{\text{ice}}^{\text{opt}}$ and optimum output speed $\omega_{\text{ice}}^{\text{opt}}$ of the ICE as follows:

$$T_{\text{ice}}^{\text{opt}} \omega_{\text{ice}}^{\text{opt}} = P_{\text{ice}}^{\text{opt}}. \tag{3}$$

By combining (1) and (3), the output power of the ICE can be controlled at the highest efficiency by changing the output torque of the ISG or the EMG. Since $P_{\text{ice}}^{\text{opt}}$ is known, the power demand on electrical system can be obtained by

$$\begin{aligned} P_{\text{ele}} = P_{\text{ice}}^{\text{req}} - P_{\text{ice}}^{\text{opt}}, \\ P_{\text{ice}}^{\text{req}} = T_{\text{ice}}^{\text{req}} \omega_{\text{ice}}, \end{aligned} \tag{4}$$

where P_{ele} denotes the power demand on electrical system and $P_{\text{ice}}^{\text{req}}$ is the power demand to the ICE.

It can distribute the power between the ISG and the EMG in the electrical system by the known parameter P_{ele}. At a certain speed, when P_{ele} is less than the peak power of the ISG, the electrical power is supplied by the ISG. While P_{ele} is up to the peak power of the ISG and less than the peak power of the EMG, the electrical power is supplied by the EMG. While P_{ele} is up to the peak power of the EMG, the electrical power is supplied by the ISG and the EMG.

It can be seen that the power distribution among the ICE, the ISG, and the EMG is very easy when using simple logic threshold approach. However, the ICE may fail to achieve the best efficiency on account of the complex nature of power-split HEV. For example, the inertial additional torque of the running/stopping of the ICE, the SOC of batteries, and

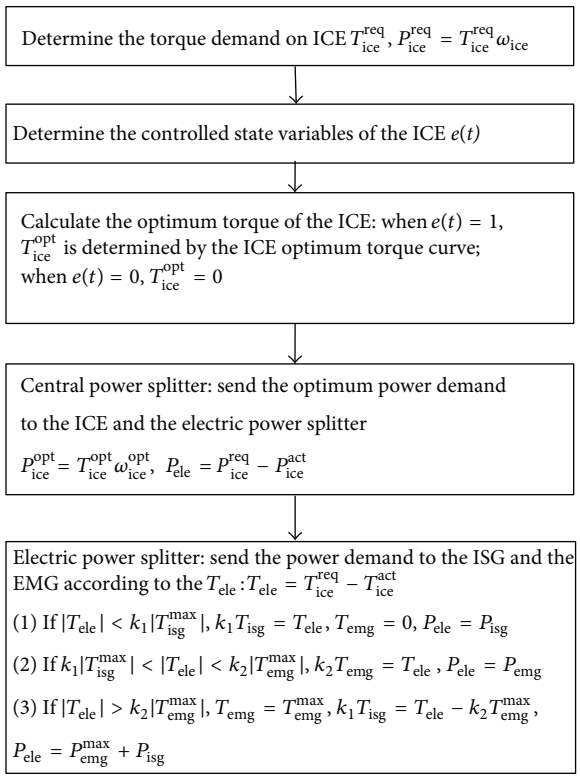

Figure 3: The control flow chart of the logic threshold approach.

the driving cycles are usually important factors affecting the ICE output. In this condition, the ICE is operating at region near the optimum torque curve. The relationship among the ICE, the ISG, and the EMG can be described as

$$\begin{aligned} k_1T_{isg} = T_{ele} = T_{ice}^{req} - T_{ice}^{act}, \quad T_{ice}^{opt} > T_{ice}^{req} > 0, \\ k_1T_{isg} + k_2T_{emg} = T_{ele} = T_{ice}^{req} - T_{ice}^{act}, \quad \text{else}, \end{aligned} \tag{5}$$

where T_{ice}^{act} is the actual output torque of the ICE and $T_{ice}^{act} \geq 0$. The power demand on electrical system P_{ele} in (4) should be changed into $P_{ele} = P_{ice}^{req} - P_{ice}^{act}$, $P_{ice}^{act} = T^{act}{}_{ice}\omega_{ice}$.

In order to give a detailed introduction of the logic threshold approach, the control flow chart is shown in Figure 3. We can see that the power distribution between the ISG and the EMG is also determined by some logic control conditions.

Equation (5) and Figure 3 reflect the actual torque distribution among the ICE, the ISG, and the EMG. One can see the logic threshold value T_{ice}^{opt} is very important to design the highest efficiency of the ICE. Because the threshold value T_{ice}^{opt} is changed into the actual output torque T_{ice}^{act}, the control strategy fails to achieve the best efficiency of the ICE. On the other hand, the electric power splitter distributes the power on the basis of the output torque of the electrical system T_{ele}, but it does not consider the efficiency of the overall electrical system. In this way, the control strategy fails to achieve the best efficiency of the system. Since simple logic threshold approach is not available to achieve the best efficiency of the system, we propose an improved logic threshold approach of energy management by taking into account the factors such as the character of ICE, the SOC, and the speed of the power-split HEV.

3. Design of the Improved Logic Threshold Approach

The control system uses an ICE logic threshold controller with three inputs and one output, where the first input is the torque demand on the ICE, the second input is the SOC, and the third input is the current ICE speed. The schematic of control system is shown in Figure 4. To design the improved logic threshold approach, we analyze the main effects of the traditional logic threshold approach. Combined with Figure 3, the main controlling parameters are the state variables of the ICE $e(t)$, the actual output torque and the power of the ICE T_{ice}^{act} and P_{ice}^{act}, and the electrical power distribution P_{ele} between the ISG and EMG. To sum up, the basic idea of the improved logic threshold approach should consider the influenced factors about the main effects and then correct the main controlling parameters to improve the efficiency of the components.

The ICE logic threshold controller calculates the torque distribution to the ICE and the first objective is the prejudgment for running/stopping of the ICE. The state running/stopping of the ICE is determined by three logic threshold values: the minimum speed demand on the ICE, the minimum torque demand on the ICE, and the current SOC, respectively. When the ICE is operating, the output speed and torque must be controlled in the peak efficiency region ($\eta_{ICE} \geq 0.35$). To ensure the efficiency, the minimum speed demand on the ICE is designed as 800 rpm and the maximum speed to the ICE is designed as 4100 rpm. On the other hand, the lowest and highest output torque of the ICE are designed as $T_{L(\omega)}$ and $T_{H(\omega)}$, respectively, as shown in Figure 2.

Next, the second objective is the calculation of T_{ice}^{act}. To calculate T_{ice}^{act}, it is very important to consider SOC of batteries firstly because SOC is related to the ICE output torque. The resistance curves and the voltage curve corresponding to SOC of the single NI-MH battery used in this study are shown in Figure 5. To ensure the batteries charging/discharging efficiency, we define that, when SOC is over 0.8, the ICE must be stopped to avoid the overcharging the batteries. When SOC is lower than 0.2, the ICE must be started to avoid the over discharge of batteries.

When SOC is in the region $[0.2, 0.8]$, the running/stopping of the ICE is determined by a binary variable, which is expressed as follows:

$$\begin{aligned} e(t-1) = 0, \quad e(t) = \begin{cases} 1, & 0.2 \leq \text{SOC} \leq 0.5 \\ 0, & \text{else}, \end{cases} \\ e(t-1) = 1, \quad e(t) = \begin{cases} 0, & 0.5 \leq \text{SOC} \leq 0.8 \\ 1, & \text{else}, \end{cases} \end{aligned} \tag{6}$$

where $e(t)$ is the binary variable, $e(t) = 0$ indicates that the ICE stops, the actual output torque is 0, and $e(t) = 1$ indicates that the ICE runs.

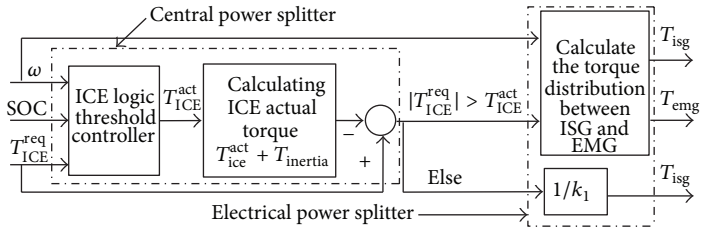

Figure 4: Schematic of control system with logic threshold controller.

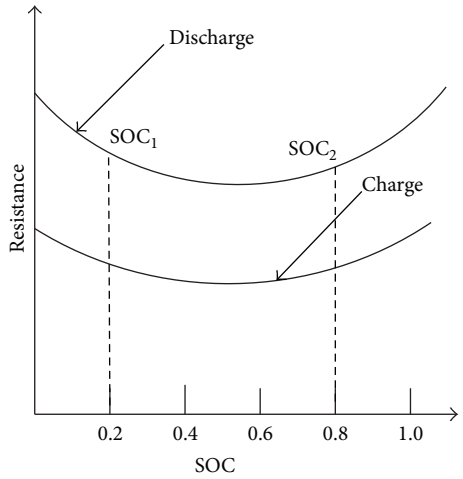

Figure 5: The resistance curves corresponding to SOC.

We can see that 0.5 can be used as a logic threshold value of SOC to change the state of ICE. However, the state of ICE may be changed quite frequently when SOC is changed in regions around SOC = 0.5. So the single logic threshold value of SOC is improved and the single value SOC = 0.5 is changed to the region [0.45, 0.55]. In this region, the state of the ICE is maintained, and the binary variable $e(t)$ is expressed as follows:

$$e(t-1) = 0, \qquad e(t) = \begin{cases} 1, & 0.2 \le \text{SOC} \le 0.45 \\ 0, & \text{else,} \end{cases}$$
$$e(t-1) = 1, \qquad e(t) = \begin{cases} 0, & 0.55 \le \text{SOC} \le 0.8 \\ 1, & \text{else.} \end{cases} \tag{7}$$

From (7), we can see that the batteries should be charged when SOC is lower than 0.45 and be discharged when SOC is more than 0.55. The ICE provides the charge or discharge power, so the actual output torque of the ICE T_{ice}^{act} must be related to the value of SOC and the modes of the vehicle.

When $e(t) = 0$, it can be known that $T_{ice}^{act} = 0$ because the ICE is turned off. When $e(t) = 1$, $T_{ice}^{act} > 0$, the calculation of T_{ice}^{act} should be determined by the modes of the vehicle. The modes of the vehicle are determined by ΔT as follows:

$$\Delta T = T_{ice}^{act} - T_{ice}^{req}. \tag{8}$$

(a) When $\Delta T > 0$ and $T_{ice}^{req} < T_{L(\omega)}$, operating the ICE within the low torque region is uneconomical. It is avoidable by activating the recharging mode so that the ICE can operate in its peak efficiency, T_{ice}^{act} can be calculated as

$$T_{ice}^{act} = T_{L(\omega)} + \frac{0.45 - \text{SOC}}{0.45 - 0.2}\left(T_{ice}^{opt} - T_{L(\omega)}\right), \quad \text{SOC} \le 0.45,$$
$$T_{ice}^{act} = T_{L(\omega)}, \quad 0.45 < \text{SOC} < 0.55. \tag{9}$$

(b) When $\Delta T < 0$ and $T_{ice}^{req} > T_{H(\omega)}$, the ICE is operated at the highest output torque by activating the hybrid mode. T_{ice}^{act} is limited as

$$T_{ice}^{act} = T_{H(\omega)}. \tag{10}$$

(c) When $\Delta T = 0$ and $T_{L(\omega)} < T_{ice}^{req} < T_{H(\omega)}$, since operating the ICE alone within the peak efficiency region is economical, the pure ICE mode is activated. T_{ice}^{act} can be calculated as

$$T_{ice}^{act} = T_{ice}^{opt}, \quad 0.45 < \text{SOC} < 0.5,$$
$$T_{ice}^{act} = T_{ice}^{req} + \frac{0.45 - \text{SOC}}{0.45 - 0.2}\left(T_{H(\omega)} - T_{ice}^{req}\right), \quad \text{SOC} \le 0.45. \tag{11}$$

When we get T_{ice}^{act}, we should consider the inertia torque of ICE to calculate the electrical system power demand P_{ele}. The relation of the power between the ICE and the electrical system can be expressed by rewriting (4) as follows:

$$P_{ele} = P_{ice}^{req} - P_{ice}^{act},$$
$$P_{ice}^{act} = \left(T_{ice}^{act} + T_{inertia}\right)\omega_{ice}, \tag{12}$$

where $T_{inertia}$ is the inertia torque of ICE, $T_{inertia} = mr^2(d\omega)/(dt)$, m is the mass of ICE flywheel, r is the radius of ICE flywheel, and ω is the angular speed of ICE flywheel.

To distribute the torque or power between the ISG and the EMG, we define a variable logic threshold value K to achieve the distribution; it is shown as follows:

$$K = \frac{P_{isg}}{P_{ele}}, \tag{13}$$

where $K = \{0, 0.1, 0.2, 0.3, 0.4, 0.5, 0.6, 0.7, 0.8, 0.9, 1\}$ and P_{isg} is the power contribution of the ISG to the electrical power demand P_{ele}. The power contribution of the EMG can be calculated as

$$P_{emg} = (1 - K) P_{ele}, \tag{14}$$

where P_{emg} is the power contribution of the EMG.

The efficiency of electrical system can be calculated as

$$\begin{aligned} \eta_{ele} &= \left\{ \frac{T_{isg}\omega_{isg}\eta_{isg}^{i} + T_{emg}\omega_{emg}\eta_{emg}^{i}}{P_{isg} + P_{emg}} \right\}^{i} \\ &= \left\{ \frac{P_{isg}\eta_{isg}^{i} + P_{emg}\eta_{emg}^{i}}{P_{ele}} \right\}^{i}, \end{aligned} \tag{15}$$

where η_{isg}^{i} is the efficiency of the ISG; η_{emg}^{i} is the efficiency of the EMG; $i = 1$ when the ISG and the EMG work in recharge state; and $i = -1$ when they work in discharge state.

By combining (13)–(15), the best efficiency $\eta_{ele\ max}$ of electrical system can be calculated as

$$\begin{aligned} \eta_{ele} &= \left\{ K\eta_{isg}^{i} + (1 - K)\eta_{emg}^{i} \right\}^{i}, \\ \eta_{ele\ max} &= \underset{K \in (K_{min}, K_{max})}{\arg\max} \left\{ K\eta_{isg}^{i} + (1 - K)\eta_{emg}^{i} \right\}^{i}. \end{aligned} \tag{16}$$

For a particular K, P_{isg} and P_{emg} can be calculated by (13) and (14). On the other hand, ω_{isg} and ω_{emg} can be obtained by knowing the wheel speed corresponding to driving cycles, η_{isg}^{i} and η_{emg}^{i}, by the calculation

$$\begin{aligned} \eta_{isg}^{i} &= f\left(T_{isg}, \omega_{isg}\right), \qquad T_{isg} = \frac{P_{isg}}{\omega_{isg}}, \\ \eta_{emg}^{i} &= f\left(T_{emg}, \omega_{emg}\right), \qquad T_{emg} = \frac{P_{emg}}{\omega_{emg}}. \end{aligned} \tag{17}$$

From (16) and (17), we can get the efficiency of electrical system to any specific K. At the same time, we can get the maximum efficiency $\eta_{ele\ max}$ by searching the maximum value of η_{ele}, then the value K corresponding to $\eta_{ele\ max}$ is used to calculate P_{isg} and P_{emg}.

From (6)~(17), the underlying reasons of the improvements can be summarized as follows: (1) the corrected $e(t)$ can reduce the running/stopping times and improve the output stability of the ICE; (2) the designed T_{ice}^{act} combined the peak region of the ICE, the modes of the vehicle, and the SOC of the batteries; it can improve the efficiency of overall vehicle control and energy management system in any modes; (3) the variable logic threshold value K can achieve the best efficiency of the electrical system.

4. Simulation and Comparative Analysis

The Urban Dynamometer Driving Schedule (UDDS) and the New European Driving Cycle (NEDC) are chosen to demonstrate the improved logic threshold approach. The important parameters of power-split HEV are listed in Table 1. The selected driving cycles are shown in Figure 6.

Table 1: Parameters of vehicles.

Component	Parameter	Power-split HEV value
ICE (Honda-Insight)	Peak power	50 kw
	Optimum torque	60 Nm
	Peak efficiency	0.4
EMG (Insight)	Peak power	30 kw
	Peak torque	±220 Nm
ISG (Insight)	Peak power	10 kw
	Peak torque	±100 Nm
NIHM battery	Voltage	288 V
	Capacity	6.5 Ah
Power-split HEV data	Radius of wheel	0.275 m
	Frontal area	1.92 m^2
	Total mass	1350 Kg

The ICE performance of the power-split HEV is shown in Figure 7. We can see that the ICE can operate in its peak efficiency region and near its optimum curve with both the logic threshold controller and the improved logic threshold controller. From Figure 7(b), the operating points of them not only behave in peak efficiency region, but also behave closer to the ICE optimum torque curve than to the ICE operating points with logic threshold controller. When the ICE is starting or running in the low speed area, some output torque points of the ICE with logic threshold controller are higher than those expected, some points even present beyond the peak efficiency region. So the operating points of the ICE with logic threshold are of less efficiency than the operating points of the ICE with improved logic threshold control.

The performances of the EMG are shown in Figures 8(a) and 8(b). It is apparent that the ICE is less efficient in two regions: (1) higher output torque in low speed and (2) lower braking torque in low speed. From Figure 8, the EMG with improved logic threshold controller behaves with higher efficiency than the ICE with logic threshold controller because it avoids the higher output torque and lower braking torque in low speed. On the other hand, the operating points of the EMG are closer to the red curve which presents the highest efficiency. So the improved logic threshold controller can improve the efficiency of the EMG. The performance of the ISG is shown in Figures 8(c) and 8(d). It should be noticed that the ISG efficiency is different from the EMG in different speed. The efficiency is higher when the ISG is operating in low output torque and low braking torque. However, the ISG is of low efficiency in high output or braking torque when it is operating at about 500 rpm. We can see that the ISG with improved logic threshold controller is operating in low output torque or braking torque region when the speed of the ISG is operating at about 500 rpm. So it avoids low efficiency in operating and higher efficiency than the ISG with logic threshold controller.

Table 2: Comparison of simulation results.

Driving cycle	ICE efficiency		The variation of the SOC (initial SOC~final SOC)		Motor driving system efficiency		Fuel consumption	
	Logic threshold	Improved logic threshold	Logic threshold	Improved logic threshold	Logic threshold	Improved logic threshold	Logic threshold	Improved logic threshold
NEDC	35.8%	37.6%	0.70~0.51	0.70~0.59	81.0%	87.1%	3.41 L	3.36 L
UDDS	34.7%	36.4%	0.70~0.47	0.70~0.56	79.5%	85.7%	3.73 L	3.64 L

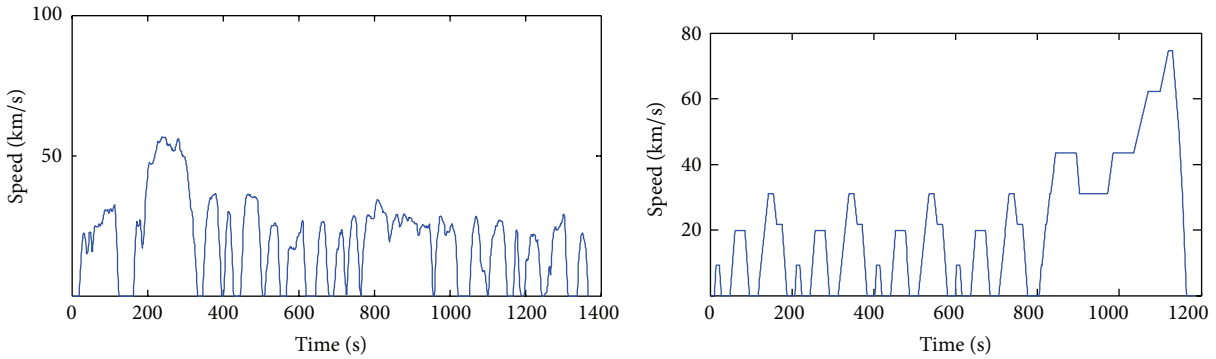

(a) UDDS (b) NEDC

Figure 6: Driving cycles.

Figure 9 shows the comprehensive results of the power-split HEV in NEDC. The torque outputs of the ICE, the ISG, and the EMG reflect that the ICE controlled by both logic threshold controller and improved logic threshold controller can work in the peak efficiency region. When the electrical system responds to high regenerative braking torque, the ISG and the EMG controlled by improved logic threshold controller can work more harmonically than logic threshold controller since the logic threshold variable K is used to achieve the torque distribution between the ISG and the EMG. In other words, it reflects the change of SOC; the initial value of SOC is set to 0.7. The final value is 0.51 when the logic threshold controller is used, but the final value is up to 0.59 when the improved logic threshold controller is used. So the improved logic threshold controller reduces the energy consumption of batteries up to 8%.

To have more specific comparative analysis, we list the ICE efficiency, the variation of SOC, and the motor driving system efficiency calculated from ADVISOR in the two driving cycles. They are shown in Table 2. We can see that the improved logic threshold controller improves the ICE efficiency and reduces the variation of SOC. The motor driving system efficiency is improved apparently. The ICE efficiency is increased by 1.7%, the fuel consumption is reduced down to 1.4%, and the motor driving system efficiency is increased by 6.1% when using the improved logic threshold controller when compared to the power-split HEV with the logic threshold controller.

5. Conclusions

This paper designs an improved logic threshold approach of energy management for a power-split HEV assisted by an ISG. By analyzing the power-split HEV structure and its operation with logic threshold approach, combining the ICE characters and the demand torque with the value of SOC to manage the ICE within its peak efficiency region, the logic threshold controller is improved. Furthermore, a variable logic threshold value K is defined to achieve the best efficiency of electrical system and achieve the power distribution between the ISG and the EMG.

Results have shown that the ICE efficiency and the efficiency of battery charging and discharging with improved logic threshold controller are improved when compared to the equally power-split HEV with the logic threshold controller. The comprehensive results show that battery power consumption reduces down to 8%, the ICE efficiency improves up to 1.7%, the fuel consumption is reduced down to 1.4%, and the motor driving system efficiency improves up to 6.1% of a power-split HEV with the improved logic threshold approach when compared with one with the logic threshold approach. The comprehensive results show the effectiveness and the validity of the improved logic threshold approach.

Acknowledgments

The authors would like to thank the anonymous reviewers for their constructive and insightful comments for further

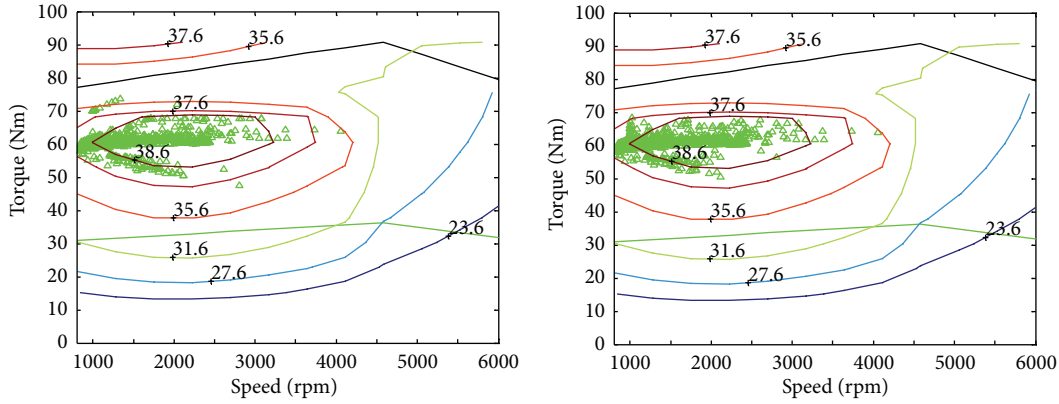

(a) Operating points of the ICE with logic threshold

(b) Operating points of the ICE with improved logic threshold

Figure 7: ICE performances in UDDS.

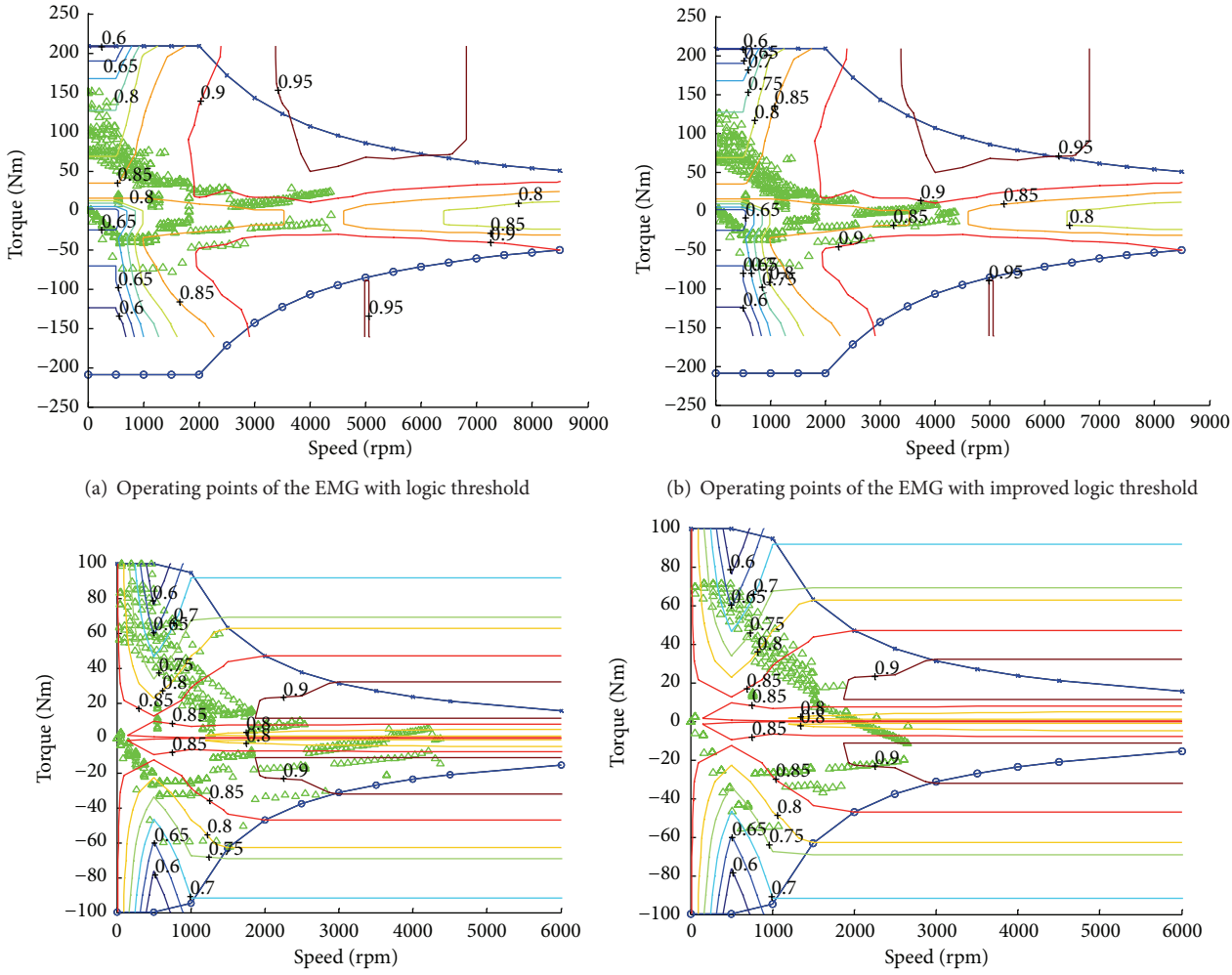

(a) Operating points of the EMG with logic threshold

(b) Operating points of the EMG with improved logic threshold

(c) Operating points of the ISG with logic threshold

(d) Operating points of the ISG with improved logic threshold

Figure 8: EMG and ISG performances in UDDS.

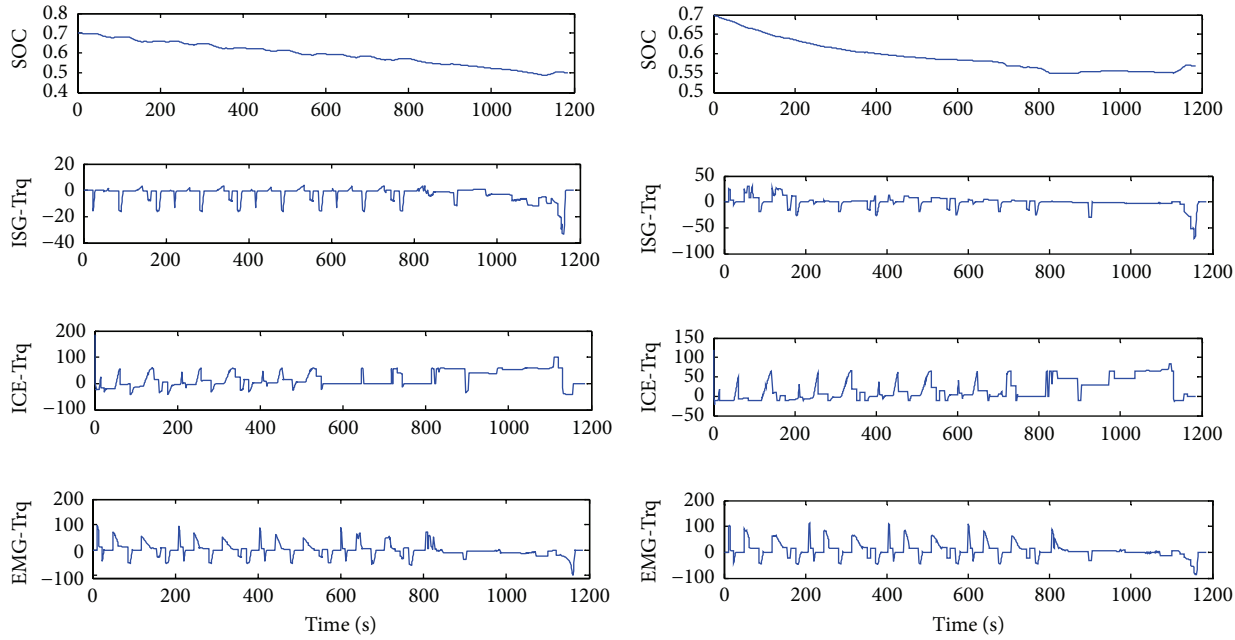

(a) Comprehensive results with logic threshold

(b) Comprehensive results with improved logic threshold

Figure 9: Comprehensive results in NEDC.

improving the quality of this paper. This work was partially supported by National Natural Science Foundation of China under Grant nos. 60904023, 51277116, and 61203047, China Postdoctoral Science Foundation under Grant no. 2013T60670, the Science and Technology Programme Foundation for the Innovative Talents of Henan Province University under Grant no. 13HASTIT038 and the Key Scientific and Technological Project of Henan Province under Grant no. 132102210247.

References

[1] H. Borhan, A. Vahidi, A. M. Phillips, M. L. Kuang, I. V. Kolmanovsky, and S. Di Cairano, "MPC-based energy management of a power-split hybrid electric vehicle," *IEEE Transactions on Control Systems Technology*, vol. 20, no. 3, pp. 593–603, 2012.

[2] L. Chen, F. Zhu, M. Zhang, Y. Huo, C. Yin, and H. Peng, "Design and analysis of an electrical variable transmission for a series-parallel hybrid electric vehicle," *IEEE Transactions on Vehicular Technology*, vol. 60, no. 5, pp. 2354–2363, 2011.

[3] F. U. Syed, M. L. Kuang, M. Smith, S. Okubo, and H. Ying, "Fuzzy gain-scheduling proportional-integral control for improving engine power and speed behavior in a hybrid electric vehicle," *IEEE Transactions on Vehicular Technology*, vol. 58, no. 1, pp. 69–84, 2009.

[4] F. U. Syed, M. L. Kuang, J. Czubay, and H. Ying, "Derivation and experimental validation of a power-split hybrid electric vehicle model," *IEEE Transactions on Vehicular Technology*, vol. 55, no. 6, pp. 1731–1747, 2006.

[5] S. Adhikari, S. K. Halgamuge, and H. C. Watson, "An online power-balancing strategy for a parallel hybrid electric vehicle assisted by an integrated starter generator," *IEEE Transactions on Vehicular Technology*, vol. 59, no. 6, pp. 2689–2699, 2010.

[6] H.-U. Rehman, "An integrated starter-alternator and low-cost high-performance drive for vehicular applications," *IEEE Transactions on Vehicular Technology*, vol. 57, no. 3, pp. 1454–1465, 2008.

[7] J. T. B. A. Kessels, M. W. T. Koot, P. P. J. van den Bosch, and D. B. Kok, "Online energy management for hybrid electric vehicles," *IEEE Transactions on Vehicular Technology*, vol. 57, no. 6, pp. 3428–3440, 2008.

[8] O. Reyss, G. Duc, P. Pognant-Gros, and G. Sandou, "Multivariable torque tracking control for E-IVT hybrid powertrain," *International Journal of Systems Science*, vol. 40, no. 11, pp. 1181–1195, 2009.

[9] A. Sciarretta, M. Back, and L. Guzzella, "Optimal control of parallel hybrid electric vehicles," *IEEE Transactions on Control Systems Technology*, vol. 12, no. 3, pp. 352–363, 2004.

[10] B. Zhang and S. Xu, "Delay-dependent Robust H∞ control for uncertain discrete-time fuzzy systems with time-varying delays," *IEEE Transactions on Fuzzy Systems*, vol. 17, no. 4, pp. 809–823, 2009.

[11] M. Montazeri-Gh and M. Asadi, "Intelligent approach for parallel HEV control strategy based on driving cycles," *International Journal of Systems Science*, vol. 42, no. 2, pp. 287–302, 2011.

[12] L. Wu, Y. Wang, X. Yuan, and Z. Chen, "Multiobjective optimization of HEV fuel economy and emissions using the self-adaptive differential evolution algorithm," *IEEE Transactions on Vehicular Technology*, vol. 60, no. 6, pp. 2458–2470, 2011.

[13] A. L. Shen, W. H. Yuan, Q. S. Zuo et al., "Intelligent optimization for logic threshold control parameter on parallel hybrid electric vehicle," *Zhongnan Daxue Xuebao*, vol. 43, no. 11, pp. 4306–4312, 2012.

[14] B. Mashadi and S. A. M. Emadi, "Dual-mode power-split transmission for hybrid electric vehicles," *IEEE Transactions on Vehicular Technology*, vol. 59, no. 7, pp. 3223–3232, 2010.

[15] J. Kim, T. Kim, B. Min, S. Hwang, and H. Kim, "Mode control strategy for a two-mode hybrid electric vehicle using electrically variable transmission (EVT) and fixed-gear mode," *IEEE Transactions on Vehicular Technology*, vol. 60, no. 3, pp. 793–803, 2011.

[16] F. Yan, J. Wang, and K. Huang, "Hybrid electric vehicle model predictive control torque-split strategy incorporating engine transient characteristics," *IEEE Transactions on Vehicular Technology*, vol. 61, no. 6, pp. 2458–2467, 2012.